



A robust two-dimensional zirconium-based luminescent coordination polymer built on V-shaped dicarboxylate ligand for vapor phase sensing of volatile organic compounds

Journal:	<i>ChemComm</i>
Manuscript ID	CC-COM-04-2018-003496.R1
Article Type:	Communication

SCHOLARONE™
Manuscripts



A robust two-dimensional zirconium-based luminescent coordination polymer built on V-shaped dicarboxylate ligand for vapor phase sensing of volatile organic compounds

Received 00th January 20xx,
Accepted 00th January 20xx

Pei-Yao Du,^{a,b,d} William P. Lustig,^b Simon J. Teat,^c Wen Gu,^{a,d} Xin Liu,^{*a,d} and Jing Li^{*b}

DOI: 10.1039/x0xx00000x

www.rsc.org/

We report herein a new two-dimensional zirconium-based luminescent coordination polymer $Zr_6(\text{sdba})_4(\mu_3\text{-O})_4(\mu_3\text{-OH})_4(\text{HCOO})_2(\text{OH})_2(\text{H}_2\text{O})_2$ (**1**) [sdba = 4,4'-sulfonyldibenzoate] exhibiting selective fluorescence responses towards a variety of volatile organic compounds upon exposure in the vapor phase. Having a unique two-dimensional signal response towards aromatic molecules, including but not limited to nitroaromatic explosives, it is capable of identification of a diverse set of analytes. In addition, compound **1** shows a remarkably high sensitivity toward acetone vapors.

The luminescent detection of analyte molecules by luminescent metal-organic frameworks (LMOFs) and luminescent coordination polymers (LCPs) is an interesting and promising field of research. This is due to the functional simplicity of luminescent detection in general, which has a fast and sensitive response and requires simple instrumentation with easy sample preparation, as well as the impressive tunability inherent in LMOFs and LCPs.¹⁻⁶ Vapor-phase fluorescence sensing in particular provides an especially practical and flexible method to detect volatile organic compounds (VOCs) and other potentially hazardous gasses and vapors. However, while extensive investigations have been made on fluorescent MOFs and CPs in solution-phase sensing over the past several years, the scope of research involving vapor phase sensing is very limited, mainly due to high exceptional sensitivity and fast response that is required for efficient vapor phase detection.⁷⁻¹¹

Volatile organic compounds comprise a broad class of materials that are present in both industrial and domestic settings. Because of their ubiquity and potential health risks, effective detection of these chemical species in the vapor phase is of high importance. Solvents, fuels, lubricants, plasticizers, and a variety of other materials can contribute to VOC exposure.¹²

One special class of VOCs are nitroaromatic compounds. The fast, effective detection of these chemicals, such as nitrobenzene (NB), 2-nitrotoluene (2-NT), and 2,4-dinitrotoluene (2,4-DNT), is an important application of vapor-phase sensing. Detection of the materials in question has substantial homeland security implications, and their accidental release from military or industrial settings poses a significant environmental risk.^{4, 13} Another important application is in the detection of common industrial solvent vapors, such as acetone. Acetone is a highly volatile substance that plays a vital role in many industrial settings and scientific laboratories. However, overexposure to acetone vapors can induce metabolic disorders and cause irreversible damage to the eyes.^{14, 15} Acetone's widespread use and miscibility with water can also pose a significant threat to the aquatic environment.

Among the reported Zr-based coordination polymers, the use of linear, ditopic carboxylate ligands has resulted in a variety of structures with a number of different applications.¹⁶⁻¹⁹ In contrast, few Zr-based coordination polymers based on flexible V-shaped dicarboxylic acids have been reported. Compared with the framework of linear aromatic ligands, a skeleton of Zr-based coordination polymers with V-shaped carboxylate acids provides structural diversity and may exhibit interesting structures and unique properties, which is worth exploring.

Herein we synthesized a new two-dimensional zirconium-based coordination polymer $Zr_6(\text{sdba})_4(\mu_3\text{-O})_4(\mu_3\text{-OH})_4(\text{HCOO})_2(\text{OH})_2(\text{H}_2\text{O})_2$ (**1** or **LMOF-601**) based on a V-shaped dicarboxylic acid, and carried out a systematic vapor phase sensing study using **1** on a broad range of analytes. While MOF-based luminescent materials have been widely explored on chemical sensing in the solution phase, to the best of our

^a College of Chemistry and Key Laboratory of Advanced Energy Materials Chemistry (MOE), Nankai University, Tianjin 300071, China.

^b Department of Chemistry and Chemical Biology, Rutgers University, 610 Taylor Road, Piscataway, New Jersey 08854, United States.

^c Advanced Light Source Lawrence Berkeley National Laboratory, Berkeley, California 94720, United States.

^d Collaborative Innovation Center of Chemical Science and Engineering (Tianjin), Nankai University, Tianjin 300071, China.

Electronic Supplementary Information (ESI) available: Experimental details, PXRD patterns, TGA, and emission spectra. CCDC 1813390. For ESI and crystallographic data in CIF or other electronic format see DOI: 10.1039/x0xx00000x

knowledge, there have been very few studies of zirconium-based coordination polymers for selective vapor-phase luminescent sensing of VOCs or explosive-related analytes.²⁰⁻²²

Upon exposure to analyte vapors, there are detectable changes in the fluorescence intensity from **1**, with both emission quenching and enhancement possible depending on the nature of the analyte. Some analytes also induce shifts in the emission wavelength, with the degree of shift varying between analytes. Taken together, these changes in intensity and frequency allow for the construction of a two-dimensional map capable of discriminating between structurally related analyte vapors. This combination of both the detection and identification of multiple analytes by a single material provides a powerful technique for environmental monitoring.^{23, 24}

Cube-shaped single crystals of **1** were prepared through a solvothermal reaction between H₂sdba and ZrCl₄ in dimethylformamide, with formic acid as the modulating agent (Fig. S1, ESI[†]). Classic Zr₆ SBUs (Fig. 1A) are linked into a 2D framework with the formula Zr₆(sdba)₄(μ₃-O)₄(μ₃-OH)₄(HCOO)₂(OH)₂(H₂O)₂, with each SBU linked to four neighboring SBUs via eight sdba²⁻ ligands. (Fig. 1b). Terminal formate ions prevent the formation of a 3D structure.

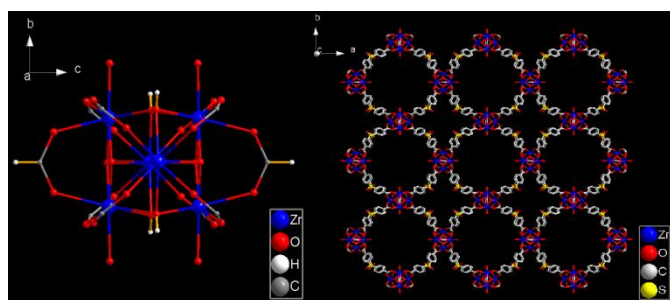


Fig. 1. (a) Zr₆ cluster in the structure. (b) 2D layer formed by Zr₆ cluster and ligand.

The crystallinity and phase purity of prepared samples of **1** were confirmed by a comparison of their experimental PXRD patterns with the simulated pattern generated from the single-crystal X-ray diffraction data of **1** (Fig. S2, ESI[†]). Thermogravimetric analysis (TGA) was also carried out to investigate the thermal stability of **1** (Fig. S3, ESI[†]).

The solid state luminescence emission spectra of free ligand H₂sdba and **1** were measured at room temperature. As shown in Fig. S4, **1** exhibited a fluorescent emission peak at 362 nm upon excitation at 285 nm. This emission peak can be assigned to a ligand-centered electronic transition.

To rapidly screen **1** for the ability to exhibit a luminescent response to various chemical species, the as-synthesized sample was suspended in ethanol and exposed to a series of solvents including H₂O, acetonitrile, methanol, 1,4-dioxane, acetone, nitrobenzene (NB), 2-nitrotoluene (NT), nitroethane (NE), nitromethane (NM) and 1-nitropropane (NP). As shown in Fig. S5, the intensity and wavelength of the emission from **1** depended heavily on the solvent that the sample was exposed to. Particularly, complete quenching (quenching efficiency > 99%) was observed only for the nitroaromatic solvents NB and NT. In the case of the three nitroaliphatic solvents (NM, NE and NP), the emission spectra show incomplete quenching with red

shifts of approximately 30 nm relative to the native LMOF. Since **1** showed strong and different luminescent responses to these solvents, it was judged appropriate to continue and test **1** for the ability to detect their vapors.

From a practicality standpoint, vapor-phase fluorescent sensors are often preferable over solution-phase sensors for detecting volatile organic compounds (VOCs), making a material with good vapor-phase performance a more meaningful sensor. To first check the potential ability of **1** to detect volatile organic compounds in the vapor phase, sensing experiments toward volatile aromatic compounds, nitroaromatic compounds, and nitroaliphatic compounds were performed. Three different categories of analyte, including aromatic compounds containing electron withdrawing nitroaromatic groups [Group-A], electron-donating groups [Group-B], and nitroaliphatic compounds [Group-C], were examined. For Group-A analytes, nitrobenzene (NB), 2-nitrotoluene (NT), and 2,4-dinitrotoluene (2,4-DNT) were selected. Group-B analytes included toluene (TO), ethylbenzene (Et-BZ), and 1,3,5-trimethylbenzene (TMB). Nitroethane (NE), nitromethane (NM), and 1-nitropropane (NP) were chosen as the Group-C analytes.

1 mL of each analyte was placed in its own small glass vial (20ml) for several days to ensure that the equilibrium vapor pressure was reached. Thin layer samples were prepared by coating a fine powder of **1** (approximately 5 mg) onto double-side tape, which was in turn mounted onto glass slides. The slides were then placed into the glass vials and exposed to the saturated vapor at room temperature. After a specified exposure time period, the slide was removed from the vial, and its solid state emission spectra was immediately collected. The response of the sensor material to any given analyte was assessed by measuring changes in the fluorescence spectra of **1** following vapor exposure. The quenching efficiency (%) was defined as $(I_0 - I)/I_0 \times 100$ where I_0 = original peak maximum fluorescence intensity and I is maximum intensity after exposure to a given analyte. The enhancement efficiency was calculated using the similar equation $(I - I_0)/I_0 \times 100$.

Impressive fluorescence quenching was observed upon exposure of sample **1** to Group-A analytes. Following a 30 minute exposure, NB quenched its emission by 46.4% (Fig. 2); with NT, a similar level of emission quench (46.8 %) was observed. 2,4-DNT showed less quenching effect, at 18.2%. While DNT contains two electron-withdrawing -NO₂ groups that increase its reduction potential and should lead to highly efficient quenching, it has a low vapor pressure and therefore limited interaction with **1**, reducing its impact (Table S2).²⁵

A considerable enhancement effect was observed for the electron-donating analytes. Toluene induced the largest emission enhancement, with 40.1% enhancement in 30 minutes. While group-C analyte vapors quenched the fluorescence of **1**, they were less efficient than nitrobenzene and nitrotoluene, despite the nitroaliphatic compounds' higher vapor pressures. This suggests that pi-pi interactions play an important part in mediating the quenching interaction between the analyte and the CP. Another possible contribution to lower quenching effect is that their LUMO energies are relative higher compared to those of nitroaromatics.⁷ The quenching trend for all three

nitroaliphatic compounds, NM>NE>NP, is in line with their respective vapor pressure, with quenching efficiencies of 22.6%, 17.2%, and 14.7% in 30 min respectively.

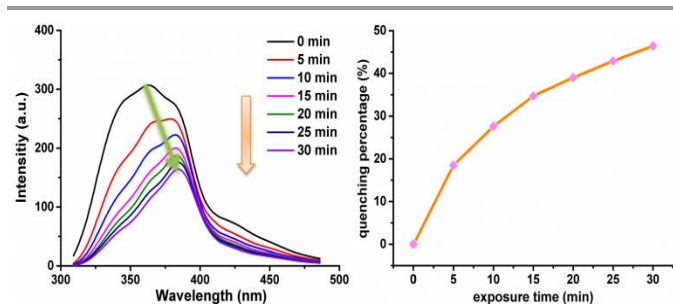


Fig. 2. The emission spectra of **1** upon exposure to NB vapor for different time periods (left), and the fluorescence quenching (%) profile of **1** as a function of time (right).

Of special note is the fact that exposure to Group-A and Group-B analyte vapors also induces shifts in the peak emission from **1**, indicating strong electronic interactions between the framework of **1** and the analytes. In contrast, the position of peak maxima in the fluorescence spectra of **1** do not change after exposure to all Group-C analytes vapors, as their aliphatic structure cannot form π - π interactions with the electron rich framework of **1**, further supporting the role these interactions play in the sensing mechanism.²⁶ By charting the fluorescence intensity change and emission frequency shift against each other, each aromatic analyte in this study can be pin-pointed on a two-dimensional map (Fig. 3).

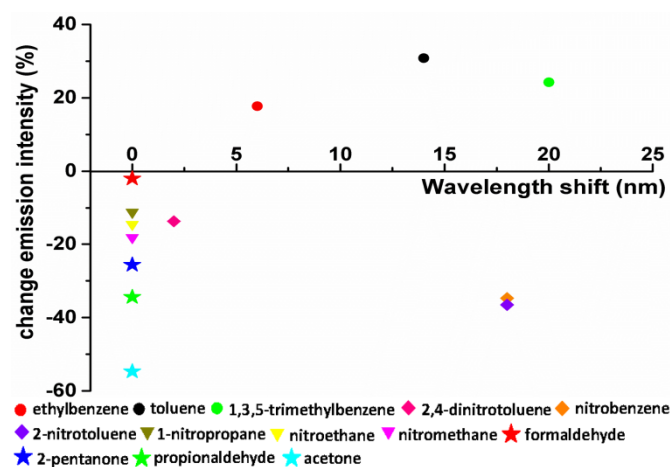


Fig. 3. A two-dimensional map based on the fluorescence response of **1** toward selected analytes. Data were taken after exposure to analyte vapor for 15 min. Some tested analytes were omitted for clarity; a 2D map of all analytes tested is given in Fig. S36.

Control experiments using an analyte-free vial did not produce any notable response (Fig. S18). Moreover, PXRD patterns of sample **1** after exposure to nitrobenzene and 2-nitrotoluene vapors are identical to the simulated pattern (Fig. S19), suggesting that the structure of **1** was highly robust under the experimental conditions and remained unchanged during the vapor sensing process. To investigate the reusability of the sensor and reversibility of the analyte-sensor interaction, a sample of **1** was rinsed with ethanol and dried at 100 °C following exposure to NB. As shown in Fig. S20, after several

cycles, the emission intensity of the sample was consistent in both the quenched and regenerated state, indicating its high stability and recyclability. This is an important consideration for the use of **1** as a reversible sensor for the detection of explosives in a practical application. These results suggest that compound **1** might be utilized as a fluorescence sensor for selectively detecting aromatic VOCs in both vapor and aqueous phases.

To investigate the mechanism of fluorescent response towards nitro-substances and other aromatics analytes, the absorption spectra of compound **1** and the emission spectra of various analytes were measured. As depicted in Fig. S21, it is observed that no spectral overlaps are attained between the absorption spectrum of **1** and the emission spectra of Group-A and Group-C analytes. However, the absorption of **1** overlaps with the emission spectra of the electron-donating analytes of group B. This permits energy transfer to move absorbed excitation energy from the analyte molecules onto compound **1**, enhancing the material's emission. In the case of the nitro-functionalized analytes, reductive energy transfer from the excited LMOF to the strongly reducing nitro analyte is an established mechanism by which these structures cause quenching in luminescent sensor materials.²⁷

Infrared spectroscopy was then utilized to confirm the interaction between **1** and analytes. Following exposure to NB and 2-NT, the IR absorbance spectrum of a sample of **1** was taken. The appearance of characteristic -NO₂ asymmetric and symmetric stretching vibrations (~1521 cm⁻¹ and ~1349 cm⁻¹) (Fig. S22 and Fig. S23) confirmed that without washing and heating, the analyte remained on the surface of the material.²⁸ Furthermore, after two days of exposure to NB vapor, **1** shows color change from white to yellow (Fig. S24).

The fluorescence response of **1** towards aldehyde and ketone vapors was also evaluated. For aldehyde analytes, benzaldehyde, formaldehyde, acetaldehyde, and propionaldehyde was selected. A series of chain and cyclic ketones was also included, comprised of cyclohexanone, cyclopentanone, 2-octanone, 2-pentanone, acetone and acetophenone. The aldehyde and ketone vapors caused a wide range of quenching responses in **1** (Fig. S35). Among all of the studied aldehyde and ketone vapors, acetone vapor is the most effective quenching agent for **1**, as the quenching percentage reaches 54.9% within 15 min (Fig. S33) suggesting that compound **1** is a potential fluorescent material for sensing of acetone vapor with a rapid response.

In other reports, acetone efficiently quenching emission usually originates from one of the following situations: (a) the collapse of the luminescent structures; (b) the absorption of the ketone by the hydrophobic pore surface of the material, where it provides nonemissive pathways for excitation recombination; (c) energy loss caused by the collision between acetone and frameworks.¹⁵ To gain further insight into the quenching process of **1** in the presence of acetone vapor, the PXRD pattern of **1** following acetone exposure was collected and compared with the simulated pattern. The two were identical. This demonstrates that the framework of **1** remained stable after exposure to acetone, and the fluorescence quenching was not ascribed to the collapse of the framework (Fig. S19). However,

IR results indicate that the acetone likely adsorbs onto the structure and affects emission in that fashion, as some characteristic peaks of **1** are indeed altered following exposure to acetone vapor (Fig. S38). The asymmetric stretching vibration of C=O group located at 1719 cm⁻¹ shifts to lower wavenumber, while new bands emerge such as C-OH stretching vibrations at 1221 cm⁻¹. These results suggest that the observed fluorescence quenching may be caused by an adsorptive interaction between acetone and the framework of **1**.

In summary, a new and highly stable zirconium-based coordination polymer constructed from a V-shaped dicarboxylic acid has been successfully synthesized. The Zr₆ clusters in the structure are linked by ligands to generate an infinite two-dimensional network. Remarkably, **1** exhibits significant fluorescence enhancement and quenching effects for electron rich and electron deficient analytes, respectively. In addition, the ability of aromatic analytes to shift the peak emission wavelength of **1** permitted the development of a 2D map which can identify a variety of analytes by the relationship between change in emission intensity and peak wavelength. The fast and effective sensing of nitroaromatic explosives and explosive related substances was achieved, and the detection of acetone and other ketone vapors by **1** was explored.

Acknowledgements

We acknowledge the financial support of the Department of Energy, Basic Energy Sciences, and Division of Materials Sciences and Engineering through Grant No. DE-FG02-08ER-46491. The Advanced Light Source is supported by the Director, Office of Science, Office of Basic Energy Sciences, of the U.S. Department of Energy under Contract No. DE-AC02-05CH11231. Pei-Yao Du, Xin Liu and Wen Gu thank the National Natural Science Foundation of China (Grant No. 21371103) and 111 Project (B12015) for their support. Pei-Yao Du gratefully acknowledges the financial support of the China Scholarship Council (CSC, 201606200043) to support her study at Rutgers University.

Conflicts of interest

There are no conflicts to declare.

References

1. P.-Y. Du, W. Gu and X. Liu, *Inorganic Chemistry*, 2016, **55**, 7826-7828.
2. P.-Y. Du, W. Gu and X. Liu, *Dalton Transactions*, 2016, **45**, 8700-8704.
3. W. P. Lustig, S. Mukherjee, N. D. Rudd, A. V. Desai, J. Li and S. K. Ghosh, *Chemical Society Reviews*, 2017, **46**, 3242-3285.
4. X. Qi, Y. Jin, N. Li, Z. Wang, K. Wang and Q. Zhang, *Chemical Communications*, 2017, **53**, 10318-10321.
5. C.-L. Tao, B. Chen, X.-G. Liu, L.-J. Zhou, X.-L. Zhu, J. Cao, Z.-G. Gu, Z. Zhao, L. Shen and B. Z. Tang, *Chemical Communications*, 2017, **53**, 9975-9978.
6. B. Li, H. M. Wen, Y. Cui, W. Zhou, G. Qian and B. Chen, *Advanced Materials*, 2016, **28**, 8819-8860.
7. S. Pramanik, C. Zheng, X. Zhang, T. J. Emge and J. Li, *Journal of the American Chemical Society*, 2011, **133**, 4153-4155.
8. Z. Hu, K. Tan, W. P. Lustig, H. Wang, Y. Zhao, C. Zheng, D. Banerjee, T. J. Emge, Y. J. Chabal and J. Li, *Chemical Science*, 2014, **5**, 4873-4877.
9. Z. Hu, B. J. Deibert and J. Li, *Chemical Society Reviews*, 2014, **43**, 5815-5840.
10. F.-Y. Yi, Y. Wang, J.-P. Li, D. Wu, Y.-Q. Lan and Z.-M. Sun, *Materials Horizons*, 2015, **2**, 245-251.
11. D.-M. Chen, N.-N. Zhang, C.-S. Liu and M. Du, *Journal of Materials Chemistry C*, 2017, **5**, 2311-2317.
12. United States EPA. Volatile Organic Compounds' Impact on Indoor Air Quality, <https://www.epa.gov/indoor-air-quality-iaq/volatile-organic-compounds-impact-indoor-air-quality>, (accessed 02/15, 2018).
13. D. Banerjee, Z. Hu and J. Li, *Dalton Transactions*, 2014, **43**, 10668-10685.
14. M. Zhao, Z.-Q. Yao, Y.-L. Xu, Z. Chang and X.-H. Bu, *RSC Advances*, 2017, **7**, 2258-2263.
15. S. Li, L. Lu, M. Zhu, C. Yuan and S. Feng, *Sensors and Actuators B: Chemical*, 2018, **258**, 970-980.
16. S. Yuan, Y.-P. Chen, J.-S. Qin, W. Lu, L. Zou, Q. Zhang, X. Wang, X. Sun and H.-C. Zhou, *Journal of the American Chemical Society*, 2016, **138**, 8912-8919.
17. J.-S. Qin, S. Yuan, A. Alsalmeh and H.-C. Zhou, *ACS Applied Materials & Interfaces*, 2017, **9**, 33408-33412.
18. D. Banerjee, W. Xu, Z. Nie, L. E. V. Johnson, C. Coghlan, M. L. Sushko, D. Kim, M. J. Schweiger, A. A. Kruger, C. J. Doonan and P. K. Thallapally, *Inorganic Chemistry*, 2016, **55**, 8241-8243.
19. Y. Wang, L. Wang, W. Huang, T. Zhang, X. Hu, J. A. Perman and S. Ma, *Journal of Materials Chemistry A*, 2017, **5**, 8385-8393.
20. F. Drache, V. Bon, I. Senkovska, M. Adam, A. Eychmüller and S. Kaskel, *European Journal of Inorganic Chemistry*, 2016, **2016**, 4483-4489.
21. Y. Zhao, Q. Zhang, Y. Li, R. Zhang and G. Lu, *ACS Applied Materials & Interfaces*, 2017, **9**, 15079-15085.
22. R. Zou, X. Ren, F. Huang, Y. Zhao, J. Liu, X. Jing, F. Liao, Y. Wang, J. Lin, R. Zou and J. Sun, *Journal of Materials Chemistry A*, 2015, **3**, 23493-23500.
23. S. Pramanik, Z. Hu, X. Zhang, C. Zheng, S. Kelly and J. Li, *Chemistry – A European Journal*, 2013, **19**, 15964-15971.
24. Z. Hu, S. Pramanik, K. Tan, C. Zheng, W. Liu, X. Zhang, Y. J. Chabal and J. Li, *Crystal Growth & Design*, 2013, **13**, 4204-4207.
25. A. Chakraborty, K. K. Ramachandran, S. S. R. K. C. Yamijala, S. K. Pati and T. K. Maji, *RSC Advances*, 2014, **4**, 35167-35170.
26. D. Banerjee, Z. Hu, S. Pramanik, X. Zhang, H. Wang and J. Li, *CrystEngComm*, 2013, **15**, 9745-9750.
27. A. Lan, K. Li, H. Wu, D. H. Olson, T. J. Emge, W. Ki, M. Hong and J. Li, *Angewandte Chemie International Edition*, 2009, **48**, 2334-2338.
28. D. V. Patil, P. B. S. Rallapalli, G. P. Dangi, R. J. Tayade, R. S. Somani and H. C. Bajaj, *Industrial & Engineering Chemistry Research*, 2011, **50**, 10516-10524.